

Insight into the Catalytic Mechanism of DNA Polymerase β : Structures of Intermediate Complexes^{†,‡}

Joseph W. Arndt,^{§,||} Weimin Gong,^{§,||} Xuejun Zhong,^{§,||} Alexander K. Showalter,^{§,||} Jia Liu,[⊥] Christopher A. Dunlap,[§] Zheng Lin,[⊥] Chad Paxson,[§] Ming-Daw Tsai,^{*,§,⊥} and Michael K. Chan^{*,§,⊥}

Departments of Chemistry and Biochemistry, The Ohio State University, 484 West 12th Avenue, Columbus, Ohio 43210

Received September 14, 2000; Revised Manuscript Received March 5, 2001

ABSTRACT: The catalytic reaction mediated by DNA polymerases is known to require two Mg(II) ions, one associated with dNTP binding and the other involved in metal ion catalysis of the chemical step. Here we report a functional intermediate structure of a DNA polymerase with only one metal ion bound, the DNA polymerase β –DNA template–primer–chromium(III)•2'-deoxythymidine 5'- β , γ -methylenetriphosphate [Cr(III)•dTMPPCP] complex, at 2.6 Å resolution. The complex is distinct from the structures of other polymerase–DNA–ddNTP complexes in that the 3'-terminus of the primer has a free hydroxyl group. Hence, this structure represents a fully functional intermediate state. Support for this contention is provided by the observation of turnover in biochemical assays of crystallized protein as well as from the determination that soaking Pol β crystals with Mn(II) ions leads to formation of the product complex, Pol β –DNA–Cr(III)•PCP, whose structure is also reported. An important feature of both structures is that the fingers subdomain is closed, similar to structures of other ternary complexes in which both metal ion sites are occupied. These results suggest that closing of the fingers subdomain is induced specifically by binding of the metal–dNTP complex prior to binding of the catalytic Mg²⁺ ion. This has led us to reevaluate our previous evidence regarding the existence of a rate-limiting conformational change in Pol β 's reaction pathway. The results of stopped-flow studies suggest that there is no detectable rate-limiting conformational change step.

DNA replication is a fundamental biological process required for cellular reproduction. The central feature of DNA replication is the template-directed nucleotidyl transfer reaction mediated by DNA polymerases. In recent years, significant progress has been made in elucidating the mechanism of enzymatic polymerization, including the determination of the structures of several DNA polymerases and their complexes with substrates or substrate analogues (1–4). These structures support a two metal ion mechanism of nucleotide incorporation, a feature thought to be shared by all families of polynucleotide polymerases (5) (Figure 1).

To decipher the microscopic events along the catalytic pathway of DNA polymerase β (Pol β)¹ as part of a larger effort to understand how DNA polymerases enhance nucleotide incorporation fidelity, we have used Cr(III) ions to experimentally distinguish the events associated with binding of each of the two metal ions. Unlike Mg(II)•nucleotide complexes which are in rapid equilibrium in aqueous solution [the exchange rate for Mg(II) is about 10^{5.2} s^{−1} (5)], Cr(III)•nucleotide complexes are relatively inert, with ligand exchange times under nonbasic conditions measured in days

[†] This work was supported by funds from The Ohio State University and the National Institutes of Health (GM43268 to M.-D.T. and AI40575 to M.K.C.). C.P. obtained fellowship support from the NSF-REU program in Chemistry at The Ohio State University. Work was done partially at SSRL, which is operated by the Department of Energy, Office of Basic Energy Sciences. The X4A beamline at the National Synchrotron Light Source, a Department of Energy facility, is supported by the Howard Hughes Medical Institute.

[‡] The coordinates have been deposited in the Protein Data Bank. PDB ID: Pol β –DNA–Cr(III)•dTMPPCP, 1huo; Pol β –DNA–Cr(III)•PCP, 1huz.

* To whom correspondence should be addressed. M.K.C.: Department of Biochemistry, The Ohio State University [phone, (614) 292-8375; fax, (614) 292-6773; e-mail, chan@chemistry.ohio-state.edu]. M.-D.T.: Department of Chemistry, The Ohio State University [phone, (614) 292-3080; fax, (614) 292-1532; e-mail, tsai@chemistry.ohio-state.edu].

[§] Department of Chemistry, The Ohio State University.

^{||} The first four authors contributed equally to this project.

[⊥] Department of Biochemistry, The Ohio State University.

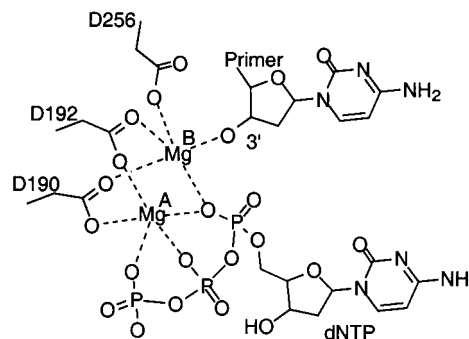
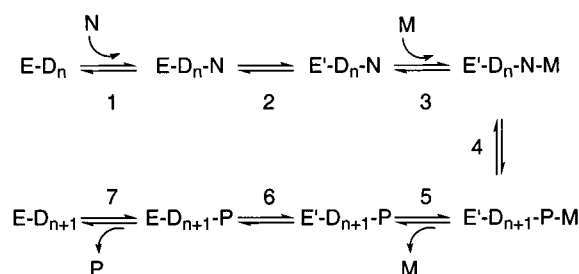


FIGURE 1: Schematic diagram of active sites showing two metal ions, the nucleotide binding ion (site A), and the catalytic ion (site B) (1, 2).

¹ Abbreviations: Pol β , *Rattus norvegicus* DNA polymerase β ; dTMPPCP, 2'-deoxythymidine 5'- β , γ -methylenetriphosphate; PCP, methylene diphosphate.

Scheme 1^a

^a E = Pol β in the open fingers conformation; E' = Pol β in the closed fingers conformation; D = DNA; N = M·dNTP; M = catalytic metal ion; P = M·PP_i.

rather than fractions of a second (6). In the absence of a free Mg²⁺ ion, Cr(III)·dTTP can induce a fast conformational change but does not proceed to the nucleotidyl transfer reaction (7). Thus, it is possible to capture the stable intermediate E'–D_n–N (Scheme 1) using the exchange-inert Cr(III)·dTTP complex.

Two major conformations of the fingers subdomain² have been observed in the crystal structures of different DNA polymerases. In free enzyme and enzyme–DNA binary complexes, the fingers subdomain was observed to adopt an “open” conformation (2, 8), with the active site freely accessible to solvent and several key catalytic residues held in salt bridges. In the corresponding enzyme–DNA–dNTP ternary complexes with two bound metal ions, the fingers subdomain adopts a “closed” conformation (1, 2) that covers the active site, due to a rotation along the “hinge” helix (helix M) that lies between the palm and fingers subdomains. The conformational change associated with the closing of the fingers subdomain has been suggested to play an important role in the fidelity of Pol β (2, 9).

The primary objective of this study is to determine the “intermediate” structures of Pol β with only one metal ion bound and to confirm the location of the Cr(III) metal ion binding site as well as to determine the overall protein conformation—whether it exists in the open form, the closed form, or a new conformation between the two. The crystal structure of the Pol β –DNA template–primer–Cr(III)·dTTPPCP is presented and shown to exist in the closed conformation. Evidence that this “intermediate” structure is indeed functional is provided by the structure of its product complex—produced by soaking of the Pol β –DNA template–primer–Cr(III)·dTTPPCP ternary complex with Mn(II) ions. Importantly, the major implication of these results is that closing of the fingers subdomain is induced by binding of M·dNTP prior to binding of the catalytic metal ion. Previous results suggested that a slow conformational change induced by binding of the catalytic metal ion was the rate-limiting step in catalysis (9). The new crystallographic results, however, suggest that the enzyme's major conformational change (closing of the fingers subdomain) is completed prior to binding of the catalytic metal ion. This has led us to

reevaluate our previous evidence regarding the existence of a rate-limiting conformational change in Pol β 's reaction pathway, a feature that has been proposed to be important to the fidelity mechanism of DNA polymerases (10). The results of stopped-flow studies suggest that there is no detectable rate-limiting conformational change step.

EXPERIMENTAL PROCEDURES

Purification of DNA Polymerase β . Recombinant rat DNA polymerase β was overexpressed in *Escherichia coli* and purified as described previously (11) with the exception that glycerol was omitted from the gel filtration column. After purification, the protein sample was washed three times in a Centricon 10 filter (Amicon) with metal-free exchange buffer [0.1 M Tris and 10 mM ammonium sulfate, pH 7.0, treated with Chelex 100 resin (Bio-Rad)], then concentrated to 30 mg/mL, and stored at –80 °C.

DNA Oligonucleotides and dTMPPCP. DNA oligonucleotides were purchased from Integrated DNA Technologies, Inc. The DNA sequences utilized for the template and primer DNA were 5'-AATAGGCGTCG-3' and 5'-CGACGCC-3', respectively. The oligonucleotides were purified via PAGE on 20% polyacrylamide–7 M urea denaturing gels and extracted with 0.1 M triethylammonium acetate, pH 7.0, and 1 mM EDTA buffer. The extracted oligos were desalted with Sep-Pak C₁₈ classic cartridges (Waters), dried in a vacuum centrifuge, and redissolved in TE buffer (10 mM Tris and 0.1 mM EDTA, pH 8.0). The concentration of the nucleotides was determined by absorbance at 260 nm. The DNA solution used for crystallization was prepared by mixing 22.5 μ L of 8 mM primer solution with 10 μ L of 16 mM template solution and then heating at 80 °C for 5 min, followed by gradual cooling to allow the template and primer to anneal.

To avoid complications from hydrolysis of the nucleotide triphosphate, the nucleotide analogue dTMPPCP (2'-deoxythymidine 5'- β , γ -methylenetriphosphate) (Amersham) was substituted. A solution of the Cr(III)·dTMPPCP complex was prepared by mixing 225 μ L of 6 mM dTMPPCP with 225 μ L of 6 mM CrCl₃ at 80 °C for 10 min (6, 12).

Crystallization of the Pol β –DNA–Cr(III)·dTTPPCP Intermediate Complex. The rat Pol β –DNA–Cr·dTTPPCP ternary complex was prepared by mixing 100 μ L of Pol β (30 mg/mL) protein solution and 20 μ L of DNA solution with 240 μ L of a Cr(III)·dTTPPCP solution. Crystals were grown by the sitting drop method from a reservoir solution (8% PEG 3350, 70 mM lithium sulfate, and 100 mM MES, pH 7.0) similar to conditions described previously (1).

Soaking Experiment. The Pol β –DNA–Cr(III)·PCP intermediate complex was prepared by soaking the crystals of the Pol β –DNA–Cr(III)·dTTPPCP ternary complex with reservoir solutions containing 40% (v/v) glycerol and 5 mM MnCl₂ for 30 min at room temperature prior to flash freezing. Longer soaking times resulted in a significant loss in the diffraction quality and the resolution of the crystals.

Data Collection. Prior to data collection, crystals were sequentially transferred to reservoir solutions containing increasing concentrations of glycerol up to a maximum concentration of 40% (v/v). Crystals were mounted on a nylon loop and then cooled in liquid nitrogen. The 2.5 and 2.6 Å resolution diffraction data sets were collected using synchrotron radiation on CCD detectors located at the

² The designation of thumb and fingers subdomains for DNA polymerase β are reversed in the nomenclatures of Pelletier et al. relative to those of Steitz et al. In our previous publications, we have followed the designation of Pelletier et al. In the present report we have switched to that of Steitz et al. because it appears to facilitate a more accurate comparison of the functionally similar structural elements in Pol β with those of other polymerases.

Table 1: Summary of Crystallographic Results

crystal	Pol β -DNA-Cr(III)-dTMPPCP	Pol β -DNA-Cr(III)-PCP
unit cell dimensions		
<i>a</i> , <i>b</i> , <i>c</i> , Å	86.1, 56.2, 105.9	85.4, 56.1, 105.8
β , deg	107.2	106.9
total/unique reflections	172244/27893	164712/33654
completeness, % ^a	88.9 (82.4)	96.6 (91.2)
<i>d</i> _{min} , Å	2.6	2.5
<i>R</i> _{sym} , % ^{a,b}	5.6 (22.4)	4.7 (30.5)
resolution range, Å	20–2.6	20–2.6
no. of non-hydrogen protein atoms	5198	5198
no. of non-hydrogen DNA atoms	616	656
no. of metal ions	2	2
no. of ligand atoms	58	18
no. of water molecules	119	123
RMS bond length dev, Å	0.015	0.020
RMS bond angle dev, deg	1.947	2.207
<i>B</i> overall, Å ²	41.91	46.86
<i>R</i> / <i>R</i> _{free} ^c	22.6/28.8	22.4/28.6

^a The numbers in parentheses are for the highest resolution shell. ^b $R_{\text{sym}}(I) = \sum_i |I_i - \langle I \rangle| / \sum_i \langle I \rangle$, where I_i is the intensity of the measurements for a reflection and $\langle I \rangle$ is the mean value for the reflection. ^c *R*_{free} was calculated on 8% of the reflections randomly omitted from the refinement.

Brookhaven National Laboratory beamline X4A and the Stanford Synchrotron Radiation Laboratory beamline 9-1. The diffraction data were processed using the programs DENZO and SCALEPACK (13).

Structure Determination and Refinement. The crystals belong to the space group *P*2₁ (Table 1) and are similar to that of the Pol β ternary complex (1) (PDB ID: 2bpg). Hence, the structures of the Pol β -DNA-Cr(III)-dTMPPCP and Pol β -DNA-Cr(III)-PCP intermediate complexes could be determined by molecular replacement. Rigid body refinement confirmed the isomorphism since both *R* and *R*_{free} factors were approximately 0.40.

Model building was performed using the program O (14), and the refinement was carried out using X-PLOR 3.851 (15) without the use of σ cutoffs. Eight percent of the data were set for the *R*_{free} factor calculation (16). A bulk solvent correction and overall anisotropic *B*-factor scaling were applied to the diffraction data. Strict noncrystallographic restraints were used in the early rounds of the refinement, but these restraints were gradually relaxed and, later, entirely removed. The Cr(III)-dTMPPCP and the Cr(III)-PCP plus the extended primer strand were modeled to the active site after removal of the restraints using $F_o - F_c$ omit maps at 3 σ . The final *R* values (*R*_{free}) were 22.6% (28.8%) and 22.4% (28.6%) for the pre- and postnucleotidyl transfer intermediates, respectively.

The average Debye-Waller factors were rather high, averaging 42 Å² in the Pol β -DNA-Cr(III)-dTMPPCP complex and 47 Å² in the Pol β -DNA-Cr(III)-PCP complex. These values, however, were similar to other published Pol β structures and have been suggested to result from inherent static disorder of the protein complex (2). The geometry was checked by PROCHECK (17), and all parameters were in the acceptable ranges with the majority being better than acceptable.

Stopped-Flow Fluorescence Assay. Kinetic experiments were performed with an Applied Photophysics SX.18MV

stopped-flow apparatus at 20 °C. The excitation wavelength was 285 nm, and the emission was monitored with a 320 nm cutoff filter (Corion) and a 0.5 mm slit width. Typical assay conditions were as follows. In one syringe, 2 μ M rat DNA polymerase β was incubated with 5 mM MgCl₂ and 0.6 μ M DNA substrate 20/36(AP)—note that AP refers to 2-aminopurine in the template strand—prepared as described previously (9). The second syringe contained 200 μ M dTTP and 5 mM MgCl₂. The reaction was initiated by mixing 65 μ L of the solution from each syringe, followed by fluorescence excitation and observation of fluorescence emission intensity as a function of time. To assign phases of emission intensity change as being associated with the chemical step or a preceding step [a conformational change (9)], a stopped-flow fluorescence experiment was performed in which ddAMP had been incorporated at the 3'-terminus, thus preventing the chemical step from occurring. The experiment was carried out by preincubating 2 μ M Pol β , 0.6 μ M 19/36(AP), 2 μ M ddATP, and 5 μ M Mg²⁺ in one syringe in order to allow ddAMP incorporation into the primer strand. The stopped-flow reaction was then initiated by mixing the dTTP and Mg²⁺ from the other syringe. Multiple experiments were performed, and the results were averaged for 6–10 runs to maximize the signal-to-noise ratio.

Turnover Assay of Intermediate Polymerase β Complex Crystals. To determine whether the crystals were of the desired intermediate, an assay was conducted as described below. Ternary complex crystals were first collected in a 0.2 μ m microfilter and then washed three times with 20 μ L of reservoir solution. The crystals were then redissolved in 60 μ L of 0.5 M MOPS, pH 7.5. Half of the sample (30 μ L) was directly heated to 90 °C for 30 min to inactivate the Pol β protein. Another half was treated with 0.5 μ L of 0.5 M Mg²⁺ for 15 min prior to heat inactivation. The two samples were then labeled with ³²P at the 5'-terminus with [γ -³²P]ATP using T4 polynucleotide kinase. The labeled samples were electrophoresed on a 20% polyacrylamide denaturing gel, and the radioactivity was quantitated using a Storm phosphorimager. The gel (provided in Supporting Information) revealed that when the crystallized Pol β ternary complex was treated with Mg²⁺, a DNA strand was obtained which was one base longer than when the complex was not treated with Mg²⁺. This confirmed that the crystallized Pol β -DNA-Cr(III)-dTMPPCP complex represents an intermediate that precedes the chemical step.

RESULTS AND DISCUSSION

Structure of Pol β -DNA-Cr(III)-dTMPPCP. Two Pol β molecules are contained in the asymmetric unit of the *P*2₁ crystal. The overall fold of the Pol β -DNA-Cr(III)-dTMPPCP structure is similar to that of the rat Pol β -DNA-Mg₂-ddCTP ternary complex (PDB ID: 2bpg) (1) (RMSD of C α atoms, 0.88 Å) and the human Pol β -DNA-Mg₂-ddCTP ternary complex (PDB ID: 2bpy) (2) structures determined previously. The protein can be divided into two basic domains. The smaller 8 kDa N-terminal domain (residues 1–87) is comprised of five α -helices and has been shown to bind single-stranded DNA and exhibit lyase activity. The larger 31 kDa catalytic domain (residues 88–335) consists of three subdomains termed the fingers, thumb, and palm (1, 18) which together form the DNA binding

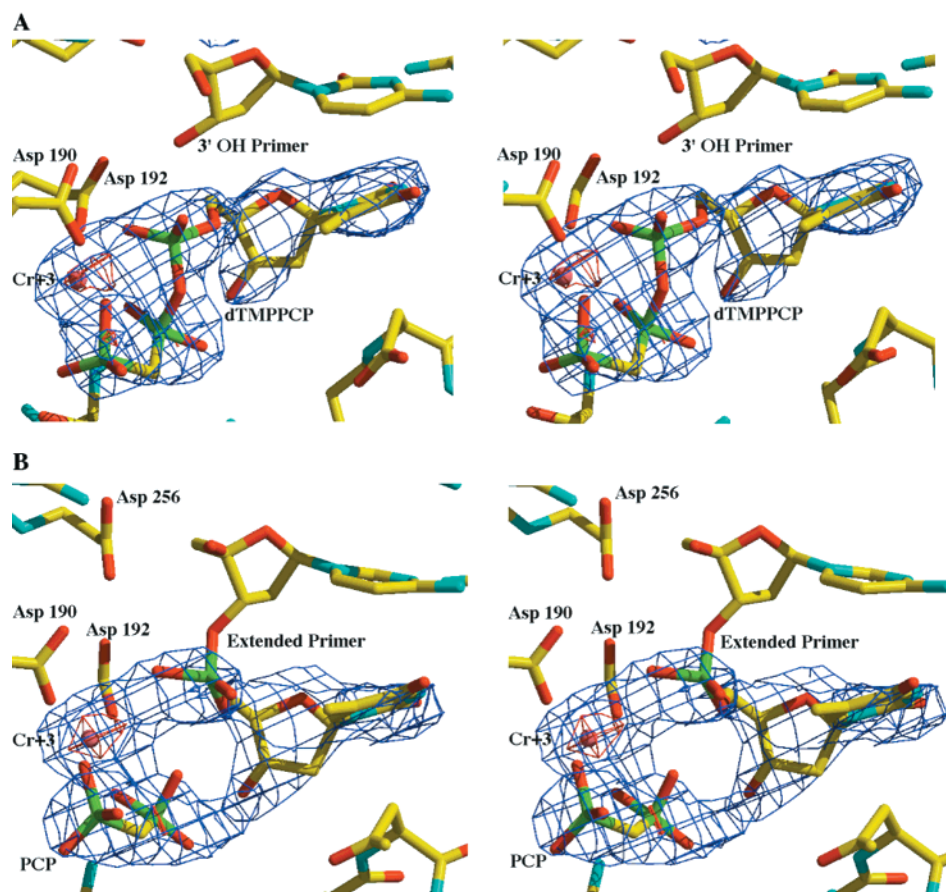


FIGURE 2: Stereoview of $F_o - F_c$ electron density maps (3σ , blue; 6σ , red) with the Cr ion and ligand omitted, superimposed on active site models. Carbon atoms are colored yellow; nitrogen, cyan; oxygen, red; phosphorus, green; and chromium, pink. (A) Pol β pre-turnover intermediate showing the presence of one Cr(III) ion and the absence of a catalytic metal ion. (B) Pol β following Mn²⁺ incubation. These figures were prepared using XtalView (27) and Raster-3D (28).

channel. Using the nomenclature of Steitz et al. (18), the 8 kDa domain leads into the thumb subdomain (residues 88–151) which is primarily α -helical, being comprised of four α -helices. The palm subdomain (residues 152–262) adopts a two-layered α/β sandwich formed from two α -helices and five antiparallel β -strands. The fingers subdomain (residues 263–335) consists of an α/β motif.

Relatively strong $F_o - F_c$ electron density (6σ) was found at metal site A in both NCS-related molecules (Figure 2A), consistent with binding of the Cr(III) ion. The metal is coordinated by the carboxylate side chains of Asp190, Asp192, and the α -, β -, and γ -phosphates of dTMPPCP. Confirming the absence of the catalytic metal ion, no electron density was observed at metal site B. The active site of the Pol β -DNA-Cr(III)-dTMPPCP structure with the electron density omitted is depicted in Figure 3B.

Previously, all ternary complex structures of DNA polymerases were obtained with a dideoxynucleotide at the end of the primer to prevent the chemical reaction. In our crystal, grown in the absence of a catalytic metal ion, it is clear that the Pol β -DNA-Cr(III)-dTMPPCP intermediate is stable with a 3'-OH at the primer terminus. Comparison of the crystal structures of Pol β complexed to DNA and Pol β complexed to DNA, Mg-ddCTP, and catalytic Mg²⁺ has previously shown that a substantial conformational change occurs after DNA binding but prior to formation of the complete Michaelis complex. It has not been known, however, whether this conformational change is induced by

binding of M-dNTP, binding of catalytic metal ion, or progressively by both of these events. The critical feature of the new Pol β -DNA-Cr(III)-dTMPPCP structure is that it adopts a closed conformation having a conformation essentially identical to that of the Pol β -DNA-Mg₂-ddCTP complex with two metal ions bound (RMSD of main chain atoms of the 31 kDa domain, 0.87 Å)—a feature distinct from the open conformation observed for Pol β -DNA binary complexes (Figure 4). This provides strong evidence that the conformational change is induced by binding of the metal-nucleotide complex and not by the binding of the catalytic metal ion.

Structure of Pol β -DNA-Cr(III)-PCP. The Pol β -DNA-Cr(III)-dTMPPCP intermediate complex was soaked with Mn(II) for about 30 min in the hope that the divalent metal would activate the crystallized enzyme, resulting in catalysis and allowing observation of a postchemistry intermediate structure. Mn(II) rather than Mg(II) was used in this study because, while both ions are capable of activating the enzyme for catalysis, the larger electron density of Mn(II) is more easily detectable—particularly in the case of partial occupancy—and thus allows a more confident determination of the absence or presence of an ion at the catalytic metal site. It is well-known that Mn(II) can substitute for Mg(II) as a catalytic activator of Pol β (11). The active site of the resulting complex structure is depicted in Figure 2B. Positive $F_o - F_c$ electron density (3σ) is found between the incoming nucleotide's α -phosphate and the 3'-oxygen of the primer

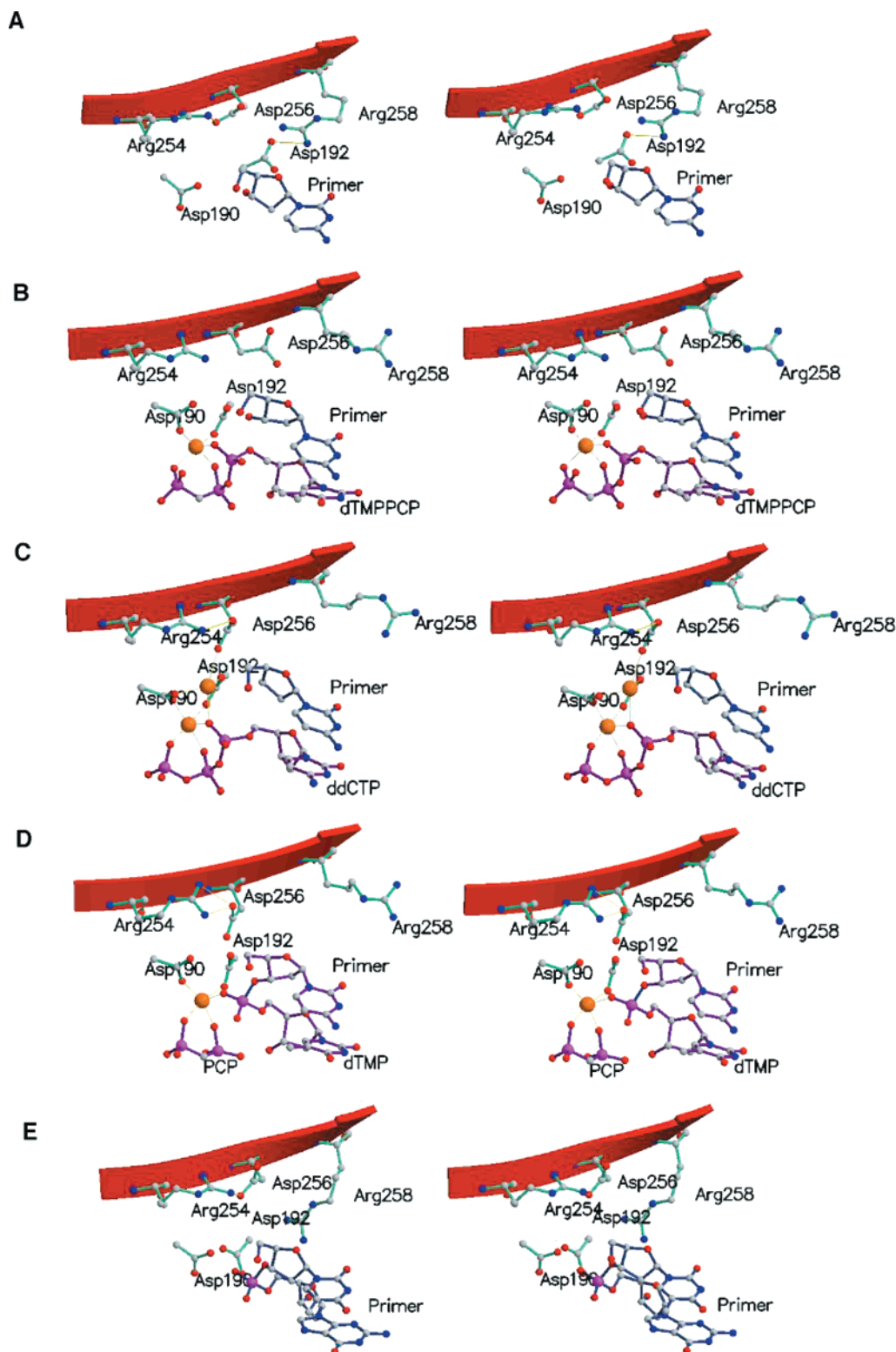


FIGURE 3: Structures of the active sites of stepwise Pol β intermediates in stereoview. (A) Structure of the human Pol β -DNA substrate binary complex (2, 10). (B) Rat Pol β -DNA-Cr(III)-dTMPPCP intermediate complex. (C) Human Pol β -DNA-Mg-ddCTP ternary complex with two Mg^{2+} ions bound (1). (D) Rat Pol β -DNA-Cr(III)-PCP intermediate complex. (E) Human Pol β -DNA product (nicked) binary complex (2). These figures were prepared using the programs MOLSCRIPT (29) and Raster-3D (28).

while no density is observed between the α - and β -phosphates, consistent with nucleotidyl transfer of the nucleotide substrate to the primer strand. Thus this structure represents a postchemistry intermediate, Pol β -DNA-Cr(III)-PCP. The nucleotide metal, Cr(III), retains coordination to the α -, β -, and γ -phosphates of the PP_i analogue (PCP) as well as to Asp190 and Asp192. No electron density is observed at the

catalytic metal site for Mn(II). In addition, the Asp256...Arg254 salt bridge, which is absent in the structure of the pre-turnover intermediate [Pol β -DNA-Cr(III)-dTMPCPP], is present in this structure, which follows the chemical step. The overall fold of the Pol β -DNA-Cr(III)-PCP intermediate structure is identical to that of the Pol β -DNA-Cr(III)-dTMPPCP structure.

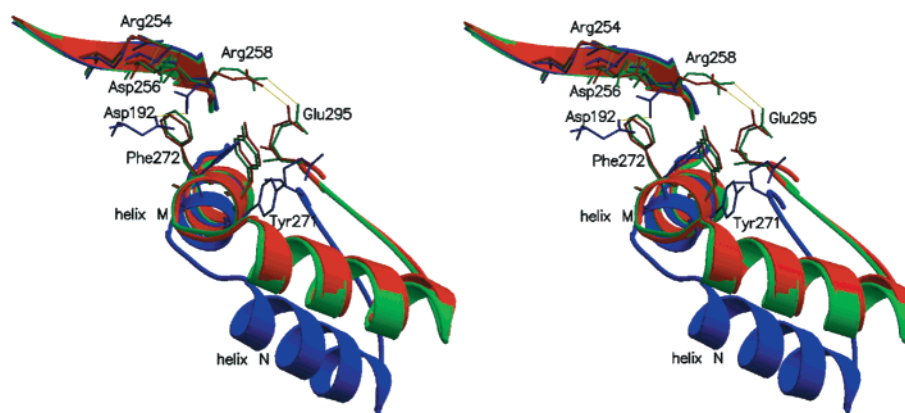


FIGURE 4: Conformational changes induced by $\text{Mg}\cdot\text{dNTP}$ binding preceding chemistry: (blue) open conformation of $\text{Pol } \beta$ based on the $\text{Pol } \beta$ -DNA binary complex (1bpx); (green) closed conformation of $\text{Pol } \beta$ based on the $\text{Pol } \beta$ -DNA- $\text{Mg}_2\cdot\text{ddCTP}$ ternary complex with two metal ions bound (1bpy); (red) closed conformation of the $\text{Pol } \beta$ -DNA-Cr(III)-dTMPPCP intermediate complex. This figure was prepared by superposition of the palm and thumb subdomains using the C_α atom of amino acids 92–273. The RMSD of the main chain atoms of helix N (amino acids 275–289) for the open $\text{Pol } \beta$ -DNA binary complex (blue) and the closed $\text{Pol } \beta$ -DNA-Cr(III)-dTMPPCP intermediate complex (red) is 7.06 Å; the RMSD for the two closed complexes (red and green) is 0.87 Å. These figures were prepared using the programs MOLSCRIPT (29) and Raster-3D (28).

Turnover in polymerase crystals has also been observed for *Bacillus* DNA polymerase (4). However, in that structure the PP_i product is released and the enzyme has translocated to the $n + 1$ position on the DNA. Turnover of $\text{Pol } \beta$ ternary complexes containing blunt-ended DNA has also been observed in other crystals of $\text{Pol } \beta$ (8). These structures are less biologically relevant, however, since they lack the template base.

The point of release of the catalytic metal ion in the polymerase reaction sequence has been previously unknown as has its association with the fingers subdomain reopening. The lack of electron density at the catalytic metal site in the $\text{Pol } \beta$ -DNA-Cr(III)-PCP structure (Figure 2B) indicates that release of the catalytic metal ion occurs immediately after the chemical step. Furthermore, the fact that the fingers subdomain reopening (a process which must occur in order to regenerate the catalyst) has not occurred in the $\text{Pol } \beta$ -DNA-Cr(III)-PCP structure suggests that this postchemistry conformational change is not induced by release of the catalytic metal. Comparison of this structure (Figure 3D) to the $\text{Pol } \beta$ -nicked DNA product structure (PDB ID: 1bpz; Figure 3E), in which the fingers subdomain has reopened (2), would suggest that opening of the fingers subdomain is induced instead by the release of $\text{M}\cdot\text{PP}_i$.

Possible Implications Presented by the Intermediate Structures. On the basis of a relatively small thio effect (11) as well as stopped-flow kinetic experiments (9), it has been suggested that a conformational change step is rate-limiting in $\text{Pol } \beta$'s reaction pathway, under processive or pre-steady-state conditions. This rate-limiting conformational change has been suggested to correspond to closing of the fingers subdomain (2). On the basis of stopped-flow kinetic evidence which suggested a $\text{M}\cdot\text{dNTP}$ -induced conformational change to be rapid relative to chemistry with a slower conformational change induced by binding of catalytic Mg(II) , we previously proposed that a rapid conformational change is induced by binding of $\text{M}\cdot\text{dNTP}$ while a slower rate-limiting conformational change is initiated by subsequent binding of the catalytic metal ion. This would presumably involve a scenario in which the observed closing of the fingers subdomain occurs in two stages—a rapid “partial” closing that follows

$\text{M}\cdot\text{dNTP}$ binding and a slow “completion” of the closing process which is induced by the catalytic metal. The structure of the $\text{Pol } \beta$ -DNA-Cr(III)-dTMPPCP complex indicates that this is unlikely, however, since there is virtually no difference in conformation between the structures prior to (Figure 3B) and after (Figure 3C) catalytic metal binding, other than rotation of the χ_1 bond in the Asp256 side chain. Further structural and functional analyses are required to resolve this dilemma, but two possible explanations are discussed below.

The first possibility is that the sequence of events suggested by crystal structures does not correspond to that suggested by kinetic analyses. One can envision that perhaps in solution the $\text{Pol } \beta$ -DNA-Cr(III)-dTMPPCP complex exists in a transient conformation between the open form and the closed form but that crystal packing forces induce it to crystallize in the closed form.

If crystal packing forces are truly a concern, however, then this issue would be relevant to all $\text{Pol } \beta$ structures published previously, since the open and closed conformations themselves have been assigned on the basis of the assumption that the $\text{Pol } \beta$ structures determined reflect their functional states. Nevertheless, our further discussion should be qualified with an awareness of this alternative interpretation of the structural results.

This leads us to the other possibility, that the kinetic model proposed previously, involving a rapid conformational change induced by $\text{M}\cdot\text{dNTP}$ and a rate-limiting conformational change induced by catalytic Mg(II) , is incorrect. Instead, the structural results presented in this paper suggest a modified catalytic model for $\text{Pol } \beta$ as shown in Scheme 1. In this scheme, step 1 is $\text{M}\cdot\text{dNTP}$ binding; step 2 is closing of the fingers subdomain induced by $\text{M}\cdot\text{dNTP}$ binding; step 3 is catalytic metal ion binding; step 4 is the chemical conversion; step 5 is the catalytic metal ion release; step 6 is opening of the fingers subdomain; and step 7 is release of $\text{M}\cdot\text{PP}_i$. The structures of $\text{E}-\text{D}_n$ (8), $\text{E}'-\text{D}_n-\text{N}-\text{M}$ (1, 2), and $\text{E}-\text{D}_{n+1}$ (8) have been solved previously. The structures reported here represent the intermediates $\text{E}'-\text{D}_n-\text{N}$ [$\text{Pol } \beta$ -DNA-Cr(III)-dTMPPCP] and $\text{E}'-\text{D}_{n+1}-\text{P}$ [$\text{Pol } \beta$ -DNA-Cr(III)- PP_i]. The specific difference between this revised

model and the model proposed previously (9) is that the “rate-limiting conformational change”, E' to E'' , does not exist. To test the validity of this possibility, we have revisited the stopped-flow kinetic experiments that provided evidence for a rate-limiting conformational change that is induced by catalytic metal binding. The results are described in the next section.

Reevaluation of the Rate-Limiting Conformational Change of Pol β by Stopped-Flow Analysis. The stopped-flow experiments referred to above involve incorporation of dTTP opposite template 2-aminopurine and monitoring of fluorescence emission (9), as has been used to study KF T4 polymerases (19). Two phases of fluorescence changes were observed, a fast phase (70 s^{-1}) and a slow phase (6 s^{-1}). The rate constant of the slow phase was comparable to k_{pol} (the pre-steady-state turnover rate constant) and could therefore reflect the chemical step or a rate-limiting conformational change. We then used a dideoxy nucleotide (ddAMP) “terminated” primer, which cannot undergo the chemical step, to differentiate between these two possibilities. Since both fast and slow phases of fluorescence change (87 and 7 s^{-1}) were still observed, we concluded that the second, slower phase reflects a rate-limiting conformational change prior to chemistry. However, the second phase in the ddAMP experiment was very weak. The weak signal on the instrument used to perform the original experiments prompted the necessity to use a 5 mm slit width on the excitation source, a condition likely to lead to photobleaching. After acquisition of a new instrument that yielded a stronger signal, it proved possible to change to a 0.5 mm slit width. Under these conditions, both experiments were repeated, and it was found that the “slow phase” in the previous ddAMP experiment is clearly absent, as shown in Figure 5. The “fast phase” is now better resolved and can be fitted by two exponentials; both are substantially more rapid than the turnover number. The result shown in Figure 5 has now been reproduced several times. We therefore conclude that the slow phase in the original ddAMP experiment was an artifact. The same experiments performed with Mn(II) rather than Mg(II) show comparable results (data not shown). This result supports the second interpretation in the previous section. It cannot be completely ruled out that there is a rate-limiting conformational change undetectable by fluorescence. However, if this is the case, the rate-limiting conformational change should involve only minor, local structural adjustments.

Feasibility and Implication of the Revised Catalytic Model. Unequivocal support for the revised catalytic model described above will require extensive and detailed kinetic analyses. However, since it is often thought that a rate-limiting conformational change is an important factor in controlling the fidelity of DNA polymerases (20), we present an argument to suggest that the fidelity can be controlled by factors other than a rate-limiting conformational change.

An induced-fit fidelity mechanism has often been invoked to explain the very low error rates of DNA polymerases (10, 20), and such an argument has been applied to Pol β (2, 9). While Fersht has shown that a conformational change cannot enhance substrate specificity relative to what is mandated at the transition state (21, 22), it has recently been suggested that Fersht's arguments are based on the assumption that the chemical step is rate-limiting, and hence the concept of induced-fit fidelity enhancement can be applied to a DNA

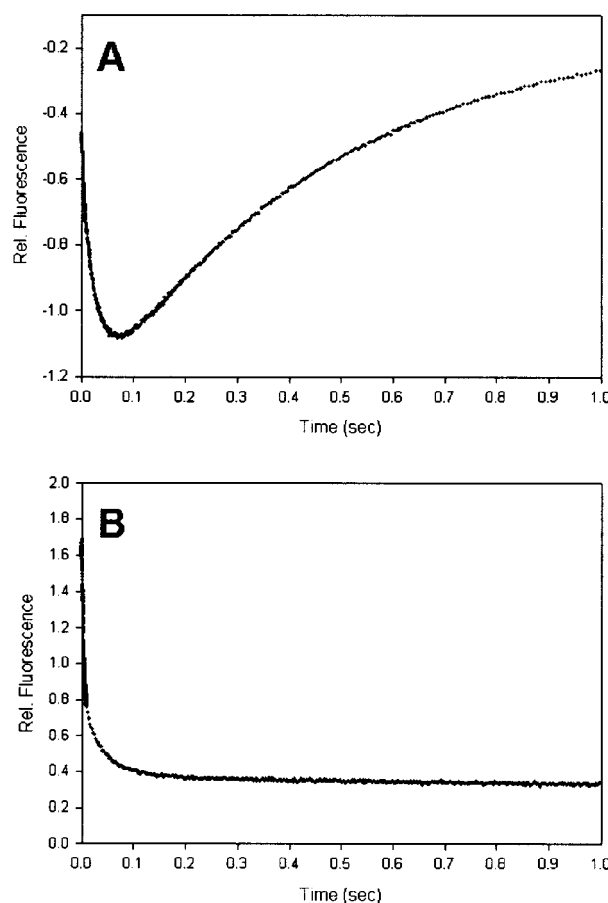


FIGURE 5: Stopped-flow fluorescence assays of Pol β . (A) Incorporation of dTTP opposite the template 2-aminopurine. In one syringe, $2\text{ }\mu\text{M}$ Pol β was incubated with $0.6\text{ }\mu\text{M}$ 20/36(AP) substrate and 5 mM Mg^{2+} . The other syringe contained $200\text{ }\mu\text{M}$ dTTP and 5 mM Mg^{2+} . The reaction was initiated by mixing $80\text{ }\mu\text{L}$ solutions from each syringe, and the fluorescence signal was monitored during the reaction. Multiple experiments were collected and averaged (9–16 runs) to improve the signal-to-noise ratio. The data were fit to a triple exponential to yield the observed rate constants of 97 ± 3.8 , 29 ± 0.56 , and $2.2 \pm 0.0087\text{ s}^{-1}$. (B) Incorporation of dTTP opposite the template 2-aminopurine with ddAMP at the 3' end of the primer. In one syringe, $2.0\text{ }\mu\text{M}$ Pol β was preincubated with $0.6\text{ }\mu\text{M}$ 19/36(AP), $50\text{ }\mu\text{M}$ ddATP, and 5 mM Mg^{2+} for 10 min to incorporate ddAMP. The reaction was initiated by mixing an equal volume of solution from another syringe containing $200\text{ }\mu\text{M}$ dTTP and 5 mM Mg^{2+} . The data were best fit to a double exponential which gave the observed rate constants (260 ± 7.8 and $44 \pm 1.4\text{ s}^{-1}$). A similar result has been reported (30) while this paper was being accepted for publication.

polymerase if the conformational change step is shown to be rate-limiting (10). Our structural and kinetic studies of Pol β suggest, however, that the conformational change is not rate-limiting.

If a conformational change step is not rate-limiting, we believe that the fidelity of Pol β could be accounted for by the selectivity of the transition state. It has been suggested that the geometry of the nascent base pair is a critical factor in determining polymerase substrate specificity, and numerous studies have supported this (3, 23). Geometry, in this sense, refers to a selection in which the size and shape of the nascent base pair are the critical properties by which the enzyme distinguishes correct from incorrect pairings. Such a selection can be realized at the transition state if the geometry of the nascent base pair must be complementary to the geometry of the active site at the transition state in

order for efficient catalysis to occur. This could be described succinctly as a difference in the transition state stabilization for different base pairs. It has been noted that Watson–Crick base pairs have a common size and shape as well as commonly positioned H-bond participators, all features that would be used for selection at the transition state. We feel that selection of this sort at the transition state may be sufficient to explain the high fidelity of Pol β (relative to that which is mandated by thermodynamic differences in the base pairs themselves). It is worthy of note that enzymatic studies with nonnatural nucleotide analogues (24) suggest that different polymerases utilize differing nucleotide properties in their selection of a correct base pair; however, we feel that this selection could be made at the transition state in all cases.

A chemical model consistent with these thermodynamic and kinetic arguments is one in which the geometry of the nascent base pair controls the placement of the catalytic metal ion. Since the metal ion located at site B (Figure 1) assists catalysis by stabilizing the buildup of negative charge at the pentacoordinate transition state, its proper placement relative to the nucleotide α -phosphate would be critical for efficient catalysis. We note that the positions and orientations of three of the primary ligands that bind the catalytic metal ion—the α -phosphate of the dNTP and the side chains of residues Asp190 and Asp192—are directly affected by the position and orientation of the incoming nucleotide. Thus M•dNTP orientation, which is a result of base pair geometry, controls the binding and placement of the catalytic metal ion. This provides one potential pathway for linkage between DNA base pairing and transition state stabilization. Put more simply, correct M•dNTP binding results in a “correct fit” for subsequent binding of the catalytic metal ion, while incorrect M•dNTP binding results in a poor fit for the catalytic Mg(II) coordination, thereby leading to less efficient turnover.

This raises a question of why the substrate-induced conformational change would be a necessary element of the reaction mechanism if it does not directly enhance the fidelity of Pol β . Such a question has been addressed in a general context (without specific reference to Pol β) previously (25). Crystallographic evidence suggests that, after the conformational change, the active site of Pol β surrounds the substrate. It appears likely that this is required to achieve maximum transition state binding and, therefore, maximum catalysis and selectivity. One important feature of an active site which surrounds substrate is that it is inaccessible to free substrate in solution (26). Without this conformational change then, the enzyme would exist exclusively in the closed, active conformation, presenting substrate binding with a large energetic barrier which would make it the rate-limiting step in the reaction. This would have the effect of substantially reducing catalytic efficiency with no effect on fidelity, which is mandated by the structure of the transition state. In this model, the nucleotide-induced conformational change does not directly enhance catalysis or fidelity of the enzyme. It

simply allows two distinct structures, one which rapidly binds substrate and one which efficiently and with high specificity catalyzes the chemical step, to coexist.

SUPPORTING INFORMATION AVAILABLE

One figure showing the polyacrylamide gel assay of radioactively labeled DNAs. This material is available free of charge via the Internet at <http://pubs.acs.org>.

REFERENCES

1. Pelletier, H., Sawaya, M. R., Kumar, A., Wilson, S. H., and Kraut, J. (1994) *Science* 264, 1891–1903.
2. Sawaya, M. R., Prasad, R., Wilson, S. H., Kraut, J., and Pelletier, H. (1997) *Biochemistry* 36, 11205–11215.
3. Doublié, S., Tabor, S., Long, A. M., Richardson, C. C., and Ellenberger, T. (1998) *Nature* 391, 251–258.
4. Kiefer, J. R., Mao, C., Braman, J. C., and Beese, L. S. (1998) *Nature* 391, 304–307.
5. Margerum, D. W., Cayley, G. R., Weatherburn, D. C., and Pagenkopf, G. K. (1978) in *Coordination Chemistry*. Vol. 2. ACS Monograph 174 (Martell, A. E., Ed.) pp 1–220, American Chemical Society, Washington DC.
6. Cleland, W. W. (1982) *Methods Enzymol.* 87, 159–179.
7. Zhong, X., Patel, S. S., and Tsai, M.-D. (1998) *J. Am. Chem. Soc.* 120, 235–236.
8. Pelletier, H., Sawaya, M. R., Wolfle, W., Wilson, S. H., and Kraut, J. (1996) *Biochemistry* 35, 12742–12761.
9. Zhong, X., Patel, S. S., Werneburg, B. G., and Tsai, M.-D. (1997) *Biochemistry* 36, 11891–11900.
10. Wong, I., Patel, S. S., and Johnson, K. A. (1991) *Biochemistry* 30, 526–537.
11. Werneburg, B. G., Ahn, J., Zhong, X., Hondal, R. J., Kraynov, V. S., and Tsai, M.-D. (1996) *Biochemistry* 35, 7041–7050.
12. Dunaway-Mariano, D., and Cleland, W. W. (1980) *Biochemistry* 19, 1506–1515.
13. Otwinowski, Z., and Minor, W. (1997) *Methods Enzymol.* 276, 307–326.
14. Jones, T. A., Zou, J. Y., Cowan, S. W., and Kjeldgaard, M. (1991) *Acta Crystallogr.* A47, 110–119.
15. Brunger, A. T. (1993) *X-PLOR Version 3.1 Manual*, Yale University, New Haven, CT.
16. Brunger, A. T. (1993) *Acta Crystallogr.* D49, 24–36.
17. Laskowski, R. A., MacArthur, M. W., Moss, D. S., and Thornton, J. M. (1993) *J. Appl. Crystallogr.* 26, 283–291.
18. Steitz, T. A., Smerdon, S. J., Jager, J., and Joyce, C. M. (1994) *Science* 266, 2022–2025.
19. Frey, M. W., Sowers, L. C., Millar, D. P., and Benkovic, S. J. (1995) *Biochemistry* 34, 9185–9192.
20. Johnson, K. A. (1993) *Annu. Rev. Biochem.* 62, 685–713.
21. Fersht, A. R. (1974) *Proc. R. Soc. London, Ser. B* 187, 397–407.
22. Fersht, A. (1983) *Enzymes: Structures and Reaction Mechanisms*, W. H. Freeman, New York.
23. Matray, T. J., and Kool, E. T. (1999) *Nature* 399, 704–708.
24. Morales, J. C., and Kool, E. T. (2000) *J. Am. Chem. Soc.* 122, 1001–1007.
25. Wolfenden, R. (1974) *Mol. Cell. Biochem.* 3, 207–211.
26. Herschlag, D. (1988) *Bioorg. Chem.* 16, 62–96.
27. McRee, D. E. (1992) *J. Mol. Graphics* 10, 44–47.
28. Merritt, E. A., and Murphy, M. E. P. (1994) *Acta Crystallogr.* D50, 869–873.
29. Kraulis, P. J. (1991) *J. Appl. Crystallogr.* 24, 945–950.
30. Shah, A. M., Li, S.-X., Anderson, K. S., and Sweasy, J. B. (2001) *J. Biol. Chem.* (in press).

BI002176J